ACADEMIC PRESS

Available online at www.sciencedirect.com

SCIENCE DIRECT®

Journal of Magnetic Resonance 161 (2003) 35–42

JMR Journal of Magnetic Resonance

www.elsevier.com/locate/jmr

Powder pattern recoupling at 10 kHz spinning speed applied to cellulose

R. Witter,* St. Hesse, and U. Sternberg

PAF, IOQ, HF, Friedrich-Schiller-Universität Jena, Max-Wien-Platz 1, 07743 Jena, Germany

Received 27 June 2002; revised 27 November 2002

Abstract

Effective powder pattern recoupling by π-pulses at spinning speeds up to 10 kHz has been introduced. In a 2D experiment, the static chemical shift spectra of the indirect dimension were separated by the isotropic values of the direct dimension. Sufficient high spinning speeds ensured optimal exploitation of spectral intensities. This experiment was used to extract the ^{13}C chemical shift tensor values of native Cellulose I and regenerated Cellulose II.

Keywords: Powder pattern recoupling; CSA recoupling; 2D iso–aniso; Cellulose; Cellulose I; Cellulose II; Bacterial cellulose

1. Introduction

The aim of this work was the extraction of the chemical shift anisotropy (CSA) information of native Cellulose I and regenerated Cellulose II, from powder patterns. First results on cellulose applying PASS [4] were presented by Hesse and Jäger [6]. The sideband analysis becomes dreadful due to the high number of overlapping lines. Well-established sideband separation techniques [1–5] are available, but they disregard intermediate motions, partial orientation, and they assume single chemical shift tensors. Therefore, we favor in this paper a contrary method which separates powder pattern like spectra. Obviously, there are only two robust sequences currently available to obtain well-resolved powder patterns with conventional hardware: PHORMAT [7] and SUPER [8]. The phase-corrected magic-angle-turning experiment (PHORMAT) employs slow rotation and synchronized pulses to produce a spinning-sideband-free isotropic-shift spectrum in the indirect dimension and the slow-spinning-sideband powder pattern spectrum, resembling the stationary-sample powder pattern, in the direct dimension. For the isotropic dimension a sufficient high number of data points has to be collected. This fact makes PHORMAT time consuming. In order to avoid this, the powder pattern evolution should proceed in the indirect dimension. This can be achieved with the experiment of Tycko et al. [9] which recouples the powder pattern spectrum by rotor-synchronous π-pulse cycles. But for this sequence the recoupling does not work satisfactory under fast spinning speed conditions. Spinning speeds higher than 5 kHz and π-pulses longer than 5 μs are not advisable. If the sample contains protons, an effective decoupling during π-pulses can be achieved by obeying the condition $\omega_{1,H}/\omega_{1,C} = 3$ [10]. Current spectrometer transmitter hardware can supply proton π-pulses down to 2 or 3 μs. If necessary the Tycko sequence can be combined with TOSS [1]. Applying the correct phase sequence, B_1 field inhomogeneities are compensated. Recently, the SUPER sequence was introduced which is very robust in respect to B_1 field inhomogeneities. SUPER works for $\omega_1 \gg \omega_r$, i.e. the spinning speed should be smaller than 10 kHz. The SUPER sequence consists out of two pulse blocks per indirect dwell time which are built from four back-to-back 180°-pulses. The phase switching of the π-pulses can be done with modern spectrometer within submicroseconds, but for some hardware configurations it causes kinds of longer pulse instabilities. Generally, it takes some more time than the phase switch needs to bring the probe circuit into stable

* Corresponding author.
E-mail address: witter@ioq.uni-jena.de (R. Witter).

1090-7807/03/$ - see front matter © 2003 Elsevier Science (USA). All rights reserved.
doi:10.1016/S1090-7807(02)00188-X

resonance. And, another disadvantage of SUPER is that it produces sheared spectra.

2. Theory

For the SUPER sequence, initial and decay transients of the individual finite 180°-pulses can be taken into account. In Fig. 1(a) the influence of some artificial spacing between the finite pulses is demonstrated by SIMPSON [11] simulations of the CSA powder pattern of the C6 site of Cellulose II. This site has one of the largest anisotropy of our samples and is regarded to be most sensitive to pulse sequence imperfections.

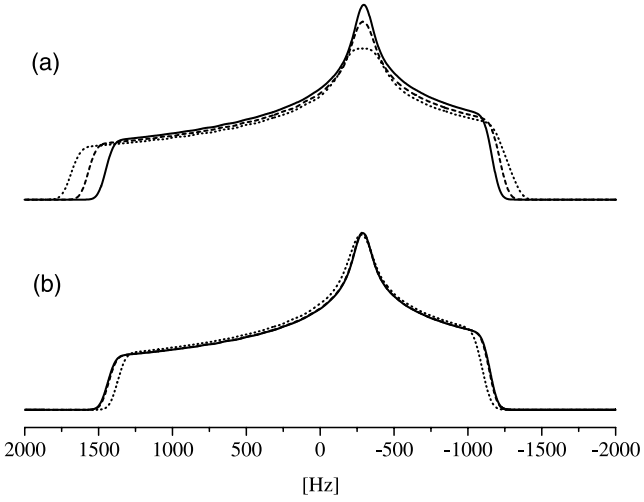

Fig. 1. CSA powder pattern SIMPSON simulation of the C6-site of regenerated Cellulose II. (a) SUPER ($T_1 = 0.25995 \times \tau$, $4 \times \pi$-pulse $= 0.14039 \times \tau$, $\chi = 0.13115$, $\tau = \tau_r$, $\omega_r = 5\,\text{kHz}$), (—) ideal pulse sequence, (––) pulses with 0.5 μs spacing, and (···) pulses with 1.0 μs spacing. (b) New sequence ($T_1 = 0.148994 \times \tau$, $T_2 = 0.398994 \times \tau$, $\chi = -0.131151$, and $\xi = 0$, $\tau = 3/2\tau_r$, $\omega_r = 10\,\text{kHz}$), (—) ideal pulses, (––) real π-pulses of 4.5 μs duration, (···) 4.5 μs pulses as well as 5% rf deviation caused by B_1 field inhomogeneities. The lines (––) and (···) in (b) are very similar and cannot be really distinguished. An artificial line broadening was added and the spectra in (b) are reversed because the scaling factor has a negative sign.

In this study, the CSA of cellulose polymorphs was measured. First, we applied the PHORMAT experiment, but we obtained a low signal to noise ratio, even after one week experimental time ($5 \times T_1 = 2\,\text{s}$). The reason is that the high resolution dimension is recorded in t_1, so that many data points have to be recorded. It was not possible to fit the obtained CSA powder patterns. Then, we applied the SUPER sequence and we could not resolve the powder patterns of the C4 and C6 carbon sites. The reason might be that the two pulse blocks have to be considered as 8 pulses instead of 2, or they may be a number between 2 and 8. This may be especially true when the effect of imperfect pulses comes more into interplay, as for some hardware configurations. Therefore, we looked for an alternative possibility and improved the 4-pulse Tycko method. The problem of the original sequence was the effect of finite pulse lengths. We decreased their influence by recoupling the chemical shift anisotropy over three rotor periods instead of one (Fig. 2). It turned out that it was even possible to use MAS spinning speeds of 10 kHz. This fact increased the spectral width of the indirect dimension and it might be also important for applications with high abundant nuclei because the homonuclear coupling can be averaged out almost completely.

The influence of real pulse lengths was investigated by numerical SIMPSOM simulations. Carbon-π pulse durations of 4.5 μs and B_1 field inhomogeneities up to 5% had only negligible influence on the line shape, see Fig. 1(b). Additionally, proton-2π pulse lengths of 4.5 μs were introduced for an effective decoupling. This technique provided undistorted separated static spectra with high signal to noise ratio. It was possible to extract the chemical shift tensors of native Cellulose I and regenerated Cellulose II at natural ^{13}C abundance.

Under magic angle spinning conditions the anisotropic contributions become time-dependent and tend to

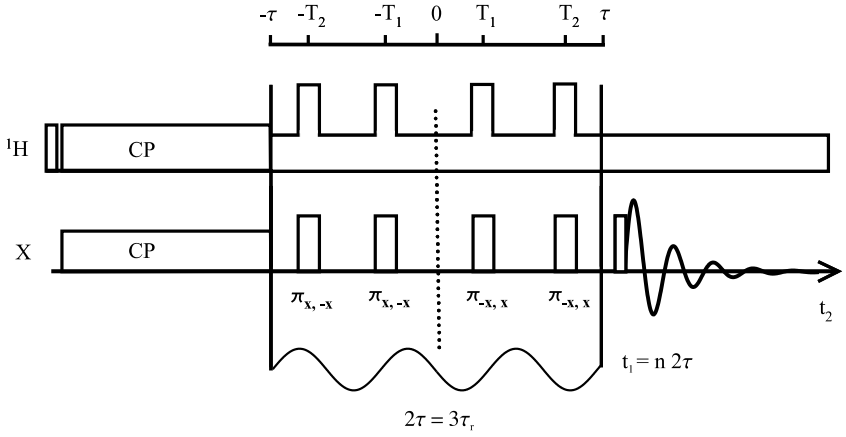

Fig. 2. 4-Pulse sequence for recoupling the CSA over three rotor periods which makes it applicable to spinning speeds of about 10 kHz.

average out. In order to achieve undistorted powder pattern recoupling, the coefficients $C_1(\Omega)$ and $C_2(\Omega)$ have to be reintroduced [9]. This can be easily understood by looking at the time-dependent chemical shift frequency in the following equation:

$$\omega(t) = \Delta\omega + C_1\cos(\omega_r t) + C_2\cos(2\omega_r t) + S_1\sin(\omega_r t) + S_2\sin(2\omega_r t). \quad (1)$$

The static case can be derived by setting the MAS rotation frequency ω_r to zero. Next we introduced a $3\tau_r$-recoupling scheme of π-pulses. To keep to the formalism of Tycko, the following conditions must be fulfilled

$$\int_0^{3\tau_r/2} f(t)\cos(\omega_r t)\,\mathrm{d}t = \int_0^{3\tau_r/2} f(t)\cos(2\omega_r t)\,\mathrm{d}t, \quad (2)$$

where $f(t)$ is a step function alternating between ± 1. This sign flipping is achieved by π-pulses, in our consideration by two pulses (4-pulse sequence) or three pulses (6-pulse sequence). The scaling factor of the powder pattern line shape becomes

$$\chi = \frac{2}{3\tau_r}\int_0^{3\tau_r/2} f(t)\cos(\omega_r t)\,\mathrm{d}t \quad (3)$$

and the offset scaling renders as

$$\xi = \frac{2}{3\tau_r}\int_0^{3\tau_r/2} f(t)\,\mathrm{d}t. \quad (4)$$

Eqs. (2)–(4) do not contain the asymmetric sine contributions, because it is automatically suppressed by a symmetric pulse sequence, see Fig. 2. With Eqs. (2)–(4) we have three conditions (I, II, III). Condition I always has to be fulfilled to ensure proper powder pattern shapes. The second condition (Eq. (3)) provides a tool for scaling the powder pattern line widths in order to fit them within the spectral window. And Eq. (4), condition III, can be used to define the shearing constant ξ. For convenience, shearing should be avoided ($\xi = 0$). First, we systematically solved the set of nonlinear equations for a 4-pulse sequence with condition I only (Fig. 3). There exists exactly one solution without shearing. The powder pattern scaling constant χ appears to be −0.13115.

In order to avoid shearing irrespective of pulse timings, a 6-pulse sequence has to be used. It can be seen that the resulting functions for timings, scaling, and shearing are only partially continuous. The functional behaviors are illustrated in Figs. 3 and 4.

We approximated the solutions of the pulse timings, the scaling factor and shearing constant as simple polynomial functions of the pulse timing (T_1/τ):

$$\frac{T_i}{\tau} = \sum_k a_k^i\left(\frac{T_1}{\tau}\right)^k, \quad i \geqslant 2,$$
$$\chi = \sum_k b_k\left(\frac{T_1}{\tau}\right)^k, \quad \tau = \frac{3}{2}\tau_r, \quad (5)$$
$$\xi = \sum_k c_k\left(\frac{T_1}{\tau}\right)^k.$$

The coefficients of the formulas (5) of the 4-pulse and the 6-pulse sequence, see Figs. 3 and 4, are given in Table 1 for appropriate continuous intervals of (T_1/τ).

The spectral width of the indirect dimension is given by

$$\Delta\omega_1 = \frac{\tau_r}{3|\chi|}, \quad (6)$$

which restricts the width of observable powder patterns. For the new 4-pulse sequence with 10 kHz spinning

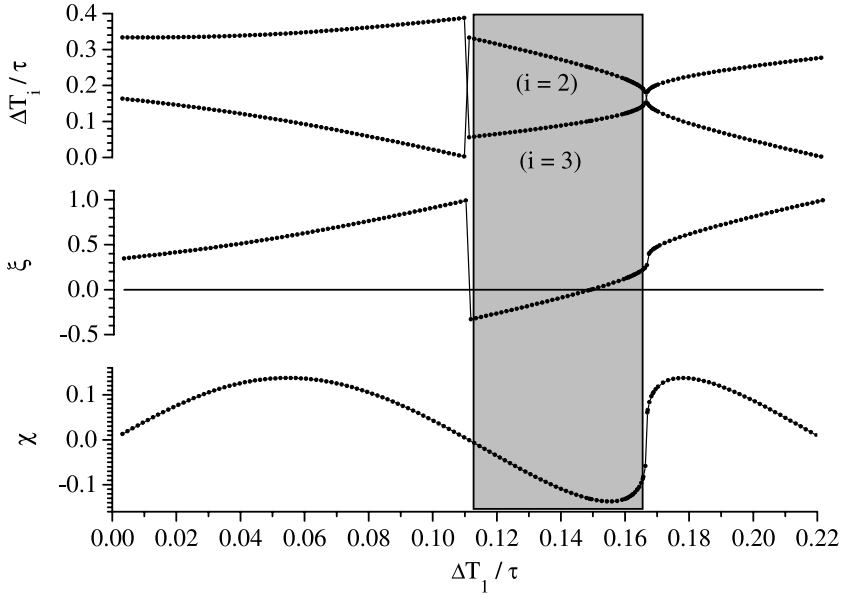

Fig. 3. Functional behavior of the pulse timings ΔT_i, shearing constant ξ and the scaling factor χ of the new 4-pulse sequence ($\Delta T_1 = T_1$, $\Delta T_2 = T_2 - T_1$, and $\Delta T_3 = \tau - T_2$). The marked range was used for parametrization of the polynomial functions, see Eq. (5).

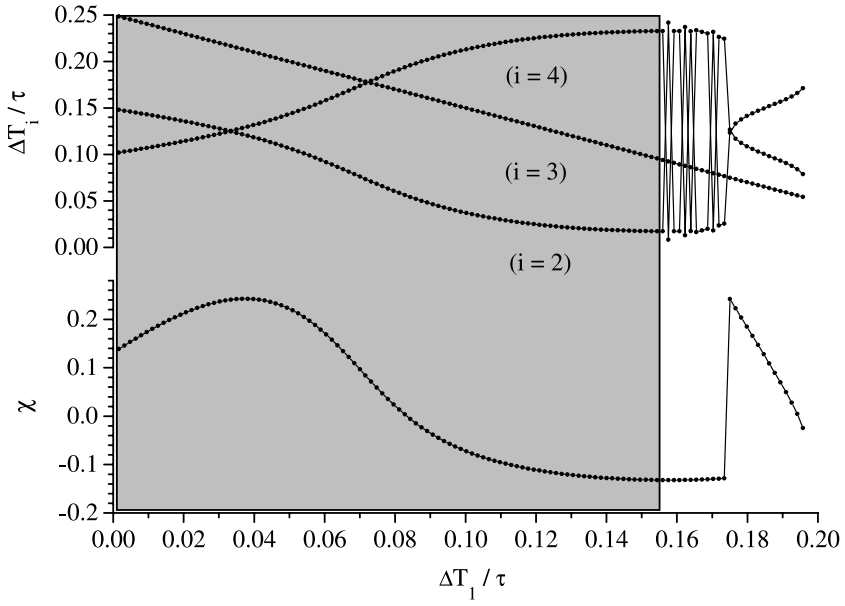

Fig. 4. Functional behavior of the pulse timings ΔT_i and the scaling factor ξ of the 6-pulse sequence ($\xi = 0$, $\Delta T_1 = T_1$, $\Delta T_2 = T_2 - T_1$, $\Delta T_3 = T_3 - T_2$, and $\Delta T_4 = \tau - T_3$). The marked range was used for parametrization of the polynomial functions, see Eq. (5).

speed and $|\chi| \approx 0.13$ the spectral width is given by roughly 25.6 kHz which is about 255 ppm for a 400 MHz spectrometer. In order to overcome these restrictions, the spinning speed can be changed and χ can be varied, either by using a sheared 4-pulse sequence, see Fig. 3, or by applying an unsheared 6-pulse sequence, see Fig. 4. Proper pulse timings can be easily calculated using Eq. (5). In Fig. 5 the influence of finite pulse lengths in respect to the powder line width is shown. The deviations between ideal patterns and theoretically predicted patterns become slightly noticeable, but they are still negligible under these conditions, especially in the case of cellulose derivatives. The SIMPSON simulations were done by integration over 2000 angle orientations (α, β, γ) with the REPULSION [12] method.

The method is restricted to powder pattern line widths bigger than the line broadening divided by $|\chi|$. Therefore, it is very important to get rid of the dipolar couplings. For the homonuclear coupling, either low nuclei abundance or sufficient MAS spinning speed is advisable. The heteronuclear coupling can be drastically

Table 1
Coefficients of the polynomial approximation of the 4-pulse sequence $(T_1/\tau) \in (0.113, 0.165)$, see Fig. 3, and the 6-pulse sequence $(T_1/\tau) \in (0, 0.155)$, see Fig. 4

k	a_k^2 of T_2	b_k of χ	c_k of ξ
4-Pulse-sequence			
0	−5.16728	+21.67778	+720.30281
1	+171.8734	−683.7583	−32323.8774
2	−1953.508	+7817.051	+602969.5055
3	+976.06	−39199.44	−5983456.05
4	−18416.94	+73696.3	+33311696.98
5	–	–	−98664146
6	–	–	+121482240
R	> 0.999		
SD	$< 10^{-4}$		
6-Pulse-sequence			
k	a_k^2 of T_2	a_k^3 of T_3	b_k of χ
0	+0.14777	+0.40149	+0.11950
1	+0.9479	−1.3431	+10.0439
2	−68.875	+51.931	−681.637
3	+3379.83	−1527.366	+33877.98
4	−86834.6	+16974.2	−891645.5
5	+1150996	−81237	+12073019
6	−8128310	+143080	−87295820
7	+29315100	–	+322899400
8	−42625000	–	−481907500
R	> 0.999		
SD	$< 10^{-4}$		

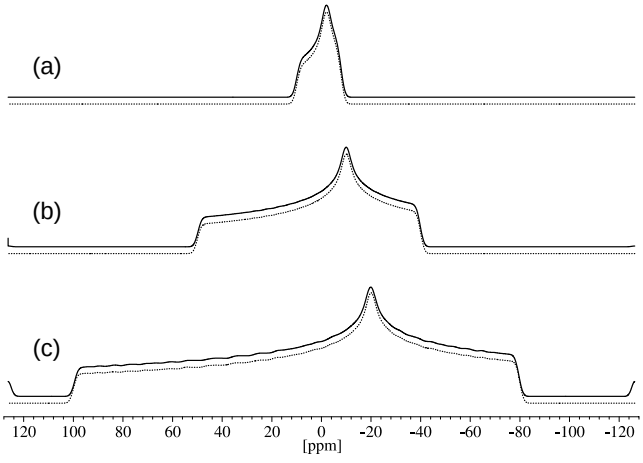

Fig. 5. SIMPSON simulations of the new sequence with different CSA powder pattern widths (···, ideal pulses; —, finite pulses of 4.5 μs). (a) $\Delta\delta = 10$ ppm; (b) $\Delta\delta = 50$ ppm; (c) $\Delta\delta = 100$ ppm, with $\eta = 0.6$ and a spectral window of about 255 ppm.

reduced by decoupling. Especially, π-pulse decoupling is achieved with the condition $\omega_{1,H}/\omega_{1,C} = 3$ [10].

3. Application

The NMR experiments were carried out on a Bruker Avance 400 MHz spectrometer with a 1 kW-proton transmitter and a Bruker MAS unit. We applied 10 kHz MAS spinning speed with 4 mm rotors which made TOSS unnecessary for our samples. Carbon π-pulse length of 4.5 μs were used. No special triggering of the pulses in respect to the rotor position was necessary. The $B_{1,H}$ field strength was chosen to hold $\omega_{1,H}/\omega_{1,C} = 1.8$. For this we obtained satisfactory powder patterns. We applied the 4-pulse sequence with zero shearing: $T_1 = 0.148994 \times \tau$, $T_2 = 0.398994 \times \tau$, and a scaling of $\chi = -0.131151$ ($\xi = 0$ and $\tau = 3/2\tau_r$). Due to the broad lines, the t_1 dimension is within the range of 16–64 data points. In order to obtain good signal to noise ratios the number of scans should be in the range of 4–1024. Then, the experimental time is in the range of minutes to days depending on the sample (T_1 in the range of seconds).

As a test for the pulse sequence, we applied our new method to conventional D-sucrose obtained from Fluka. The structure of this carbohydrate is known from neutron diffraction studies [13] and a single crystal NMR investigation was performed by Sherwood et al. [14]. The authors assigned the 12 carbon resonances to the crystallographic sites as presented in Table 2. This assignment is adopted throughout our work.

The iso–aniso spectrum of sucrose, obtained with our method, is presented in Fig. 6. It shows 1D slices only for five sites, but the spectral resolution and high signal to noise ratio allowed the extraction of the principal values of all 12 tensors with a fitting error smaller than 3 ppm. The analysis was done using the powder pattern fit routine of Dmfit [15]. We compared our experimentally determined CSA information of sucrose with the single crystal measurements of Sherwood et al. [14], see Table 2. The standard deviation to the single crystal investigation is 4.5 ppm. The largest difference is up to 10 ppm (C5 position) (see Fig. 6).

Natural polymers, as native bacterial cellulose and regenerated cellulose, consist of long chains of (1–4) linked β-D-glucopyranose units and form fibrous structures with crystalline and non-crystalline domains. The major polymorphs are native Cellulose I and the regenerated polymorph form II. Among these ordered forms the polymorph II is most intensely investigated by diffraction methods, and several crystal structures have been proposed. According to the X-ray studies of Kolpak and Blackwell [16], Cellulose II consists of two antiparallel chains of β-D-glucopyranose units and contains four monomer units per unit cell. This result was confirmed by a recent neutron diffraction study, but another orientation of the C(6)–OH group was proposed leading to a different hydrogen bond system [17]. In the case of native cellulose the discussion about the atomic structure of this polymorph was revived in 1984, when Atalla and VanderHart proposed two phases for native Cellulose I based on results obtained by solid-state ^{13}C CP–MAS NMR experiments [18–20]. Consequently, it is now established that the polymorph I can be subdivided in the phase most abundant in lower plants and bacteria (the Iα phase) and in the Iβ phase abundant in higher plants [18–22]. The structure of these two phases was resolved by Sugiyama et al. [21] using electron diffraction.

VanderHart and Atalla [19] published a first assignment for the resonances of C(1) (96–108 ppm), C(4) (81–93 ppm), and C(6) (60–70 ppm). The cluster of signals between 70 and 80 was attributed to the sites C(2), C(3), and C(5). This assignment including the carbon–carbon connectivity was readily confirmed by solid-state INADEQUATE NMR [23]. Finally, an assignment of all

Table 2
^{13}C chemical shift anisotropy principal values of D-sucrose from Fig. 5

Carbon	Experiment				Sherwood et al. [14]			
	δ_{11}	δ_{22}	δ_{33}	δ_{iso}	δ_{11}	δ_{22}	δ_{33}	δ_{iso}
C1	74.4	90.8	115.3	93.5	69.1	89.1	123.8	94.0
C2*	90.5	77.1	54.6	74.1	94.2	74.5	53.6	74.1
C3*	88.7	73.2	56.7	72.9	91.8	73.3	53.6	72.9
C4	84.0	73.1	47.0	68.0	86.0	77.1	40.7	67.9
C5*	90.3	75.9	54.6	73.6	93.7	82.8	44.2	73.6
C6*	79.5	66.7	34.7	60.3	86.3	67.2	28.1	60.5
C1′	86.4	72.1	40.7	66.4	87.1	74.4	38.0	66.5
C2′	92.8	100.5	114.7	102.7	89.9	97.7	120.6	102.7
C3′	70.5	79.2	99.3	83.0	68.5	77.4	104.1	83.3
C4′	51.3	67.6	97.1	72.0	46.7	66.1	103.6	72.1
C5′	100.6	90.6	54.8	82.0	105.5	92.2	48.4	82.0
C6′	82.2	67.4	34.5	61.4	84.3	69.8	29.8	61.3

We labeled the carbon sites analogue to Sherwood et al. [14] Tensor values are ordered according the convention: $|\delta_{33} - \delta_{iso}| \geqslant |\delta_{11} - \delta_{iso}| \geqslant |\delta_{22} - \delta_{iso}|$. The standard deviation between the tensor values of both methods turned out to be 4.5 ppm. The carbon sites indicated by a star are comparable with the corresponding cellulose sites (see Table 3).

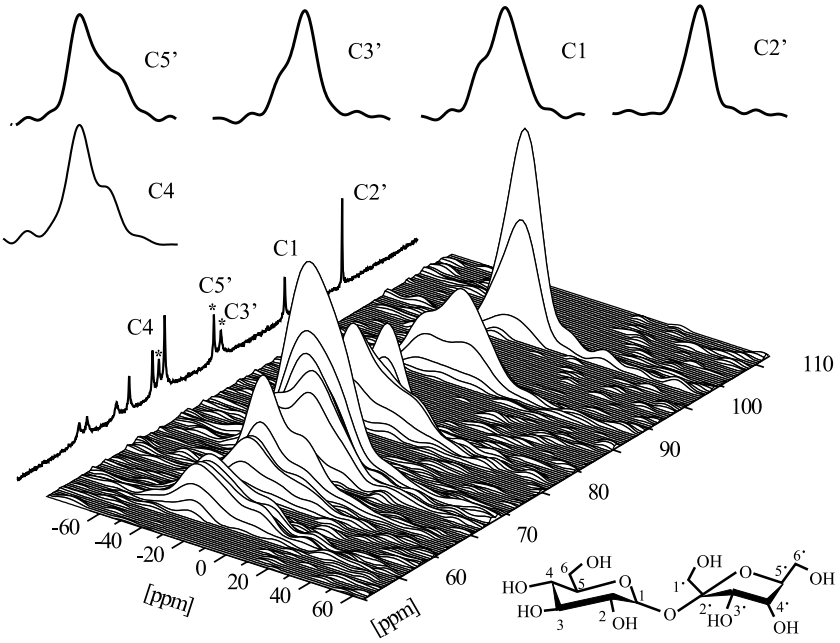

Fig. 6. 2D spectrum and five extracted 1D powder pattern slices of sucrose. The spectrum was obtained within 38 h (32 t_1 data points, 216 scans, 20 s repetition time).

six carbons of Cellulose Iα and Iβ were given by Erata et al. [24] and Kono et al. [25]. Within this paper, these assignments are adopted, and the resonances of Cellulose II are assigned in analogy to Cellulose I (see Fig. 7).

Some resonances of the crystalline Cellulose II domains display a clear splitting into two components, caused by the origin chain and the center chain, the last denoted with a prime. But up to now, it is not possible to resolve all 12 resonances in Cellulose II. According to Sugiyama et al. [21,22], Cellulose Iα contains only one chain per unit cell but two glucose residues which are denoted by subscripts in Table 3. In the case of bacterial cellulose one should observe 12 resonances of the Iα polymorph and 24 low intensity resonances of the Iβ polymorph. But despite the good spectral resolution not all resonances could be resolved. The complete assignment is deduced from theoretical calculations [26,27] (see Figs. 8 and 9).

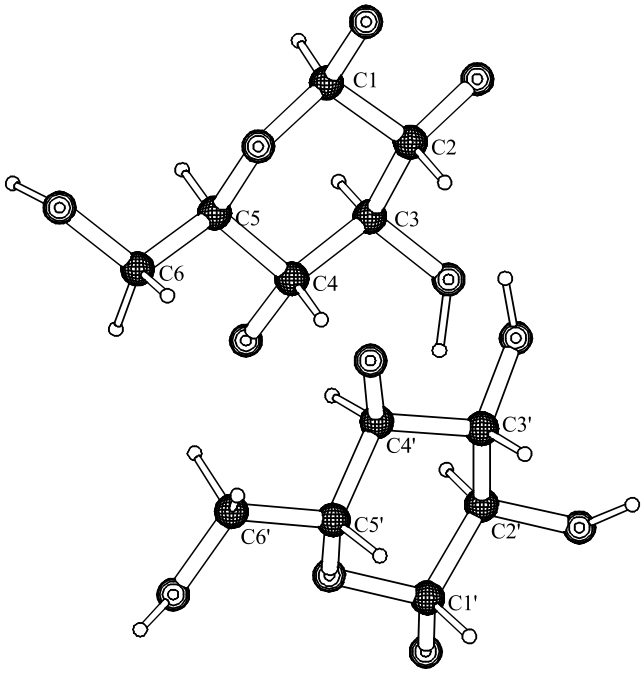

Fig. 7. The unit cell of Cellulose II contains four glucose units of two chains: origin chain and center chain according to Kolpak et al. (the center chain is denoted with a prime). The asymmetric unit consisting of two glucose units is shown.

4. Summary and conclusion

For the first time, the chemical shift tensor values of Cellulose I and II were obtained experimentally by a powder pattern method at natural ^{13}C abundance. The C4 and C6 carbon sites have the largest chemical shift anisotropies reaching about 30 ppm. Generally, it turns out that the anisotropies are in most cases much smaller than their theoretical predictions in Koch et al. [26] Due to structural similarities the C2, C3, C5, and C6 sites of sucrose are comparable with the corresponding cellulose sites which can be seen by comparison of Tables 2 and 3. Although the cellulose samples contain mostly crystalline components, the resonances C1, C2, C3, and C5 overlap with amorphous contributions (~5%), and hence the powder pattern line shapes are not as good as for sucrose. For our bacterial cellulose about 25% of the β-phase overlap with about of 75% of the α-phase.

Table 3
CSA tensor values of native Cellulose I and regenerated Cellulose II according to Figs. 7 and 8

Carbon	δ_{iso}	δ_{11}	δ_{22}	δ_{33}	$\Delta\delta$	η
Naturally built Cellulose Iα						
C1$\alpha_{1,2}$	105.5	116.9	106.4	93.2	−12.3	0.85
C4α_1	90.2	104.5	98.8	67.4	−22.8	0.25
C4α_2 (C4$\beta_{1,2}$)*	89.3	104.4	97.8	65.8	−23.5	0.28
C3α_1	75.0	88.0	76.7	60.3	−14.7	0.77
C3α_2 (C3′$\beta_{1,2}$)*	74.5	88.1	76.4	59.0	−15.6	0.75
C5α_1 (C5$\beta_{1,2}$)*	72.9	90.4	79.7	48.6	−24.3	0.44
C2α_1 (C2$\beta_{1,2}$, C2′$\beta_{1,2}$, C5′$\beta_{1,2}$)*	72.0	87.6	74.1	54.3	−17.7	0.76
C2α_2, C5α_2	71.1	87.4	74.8	51.1	−20.1	0.63
C6$\alpha_{1,2}$ (C6$\beta_{1,2}$, C6′$\beta_{1,2}$)*	65.6	85.2	73.2	38.4	−27.2	0.44
Naturally built Cellulose Iβ						
C1$\beta_{1,2}$	106.2	118.0	106.8	93.9	−12.3	0.91
C1′$\beta_{1,2}$	104.2	116.3	104.6	91.7	−12.5	0.93
C4′$\beta_{1,2}$	88.5	103.4	96.5	65.6	−22.9	0.30
C3$\beta_{1,2}$	76.0	89.6	78.1	60.3	−15.7	0.73
Regenerated Cellulose II						
C1	107.3	119.2	107.7	94.9	−12.4	0.93
C1′	105.4	119.1	105.5	91.7	−13.7	0.99
C4	89.0	106.1	97.8	63.0	−26.0	0.32
C4′	87.8	107.2	98.0	58.3	−29.6	0.31
C3, C3′	76.9	64.1	76.2	90.5	13.6	0.89
C5, C5′	75.0	92.5	76.8	55.6	−19.4	0.81
C2, C2′	73.2	89.9	75.4	54.3	−18.9	0.77
C6, C6′	62.7	85.6	68.4	34.1	−28.6	0.60

The prime indicates the center chain. Used tensor convention: $|\delta_{33}-\delta_{iso}| \geqslant |\delta_{11}-\delta_{iso}| \geqslant |\delta_{22}-\delta_{iso}|$, $\Delta\delta = \delta_{33}-\delta_{iso}$, and $\eta = (\delta_{22}-\delta_{11})/\Delta\delta$.
* Sites supposed to overlap with the main resonances are given in parentheses.

Considering the experimental error of 4.5 ppm it is obvious that most differences are within this range. The largest deviations are observed at the C5α_1, C5α_2, and C4, C4′ sites. This might be due to different conformations in respect to the hydroxymethyl group which should mainly influence the magnetic shielding of C4, C5, and C6 sites.

For a further improvement of the experiment, which makes it usable for even higher spinning speeds and anisotropies, the influence of real pulse forms and du-

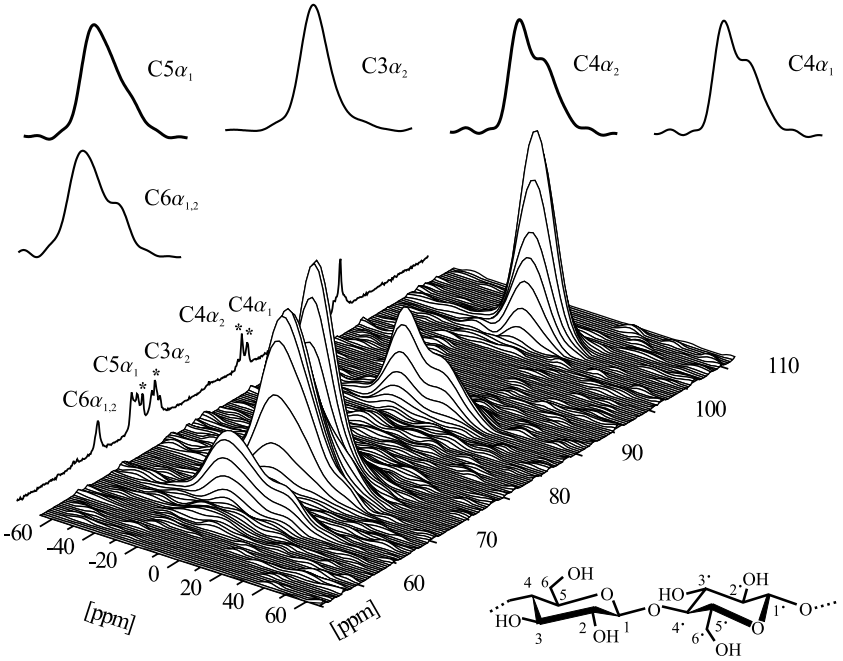

Fig. 8. 2D spectrum and five extracted powder pattern spectra of bacterial cellulose, containing mainly Cellulose Iα. The spectrum was obtained within roughly 18 h (32 t_1 data points, 1024 scans, 2 s repetition time).

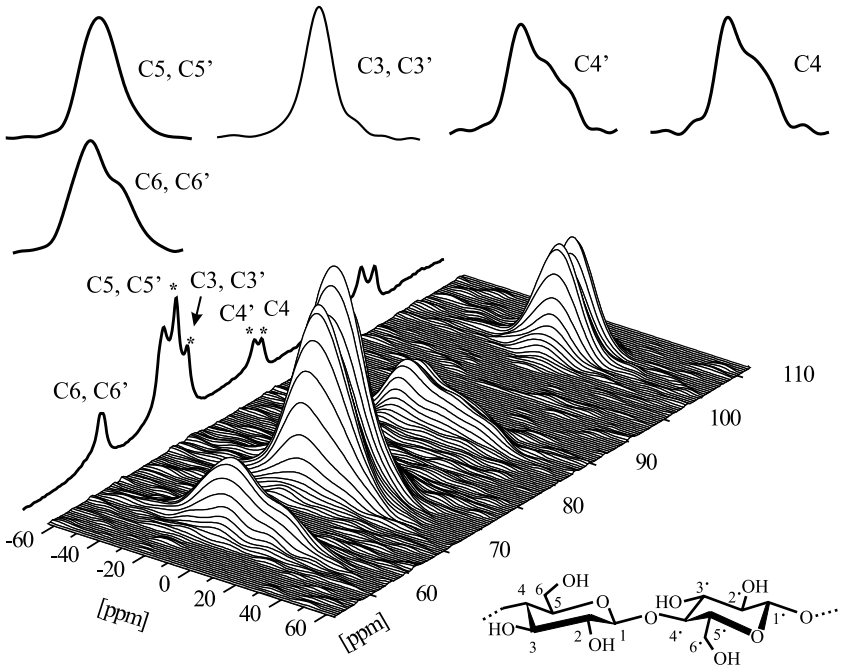

Fig. 9. 2D spectrum and five extracted powder pattern slices of regenerated Cellulose II. The spectrum was obtained within roughly 18 h (32 t_1 data points, 1024 scans, 2 s repetition time).

rations have to be taken into account. If the ratio ω_{1H}/ω_{1C} could be larger than 2, better proton decoupling would be possible, improving the quality of the powder patterns. Otherwise, Cellulose I samples with higher content of Cα or Cβ phase should be used.

Acknowledgments

This work was funded by the Sonderforschungsbereich 436 "Metal mediated reactions modelled after nature" and the DFG project "Cellulose and cellulose derivatives: molecular and supramolecular structure design." The authors acknowledge the Technische Universität Chemnitz, especially Prof. Dr. Stefan Spange and Dr. Hardy Müller for providing the Bruker Avance 400 spectrometer, as well as the groups of Prof. Dr. Dieter Klemm (Uni Jena) and Prof. Dr. Gerhard Wegener (Uni Munich) for sample preparation. We thank Dr. Detlef Reichert and Prof. Dr. Gerhard Scheler for private communications.

References

[1] W.T. Dixon, J. Chem. Phys. 77 (1982) 1800.
[2] H. Geen, G. Bodenhausen, J. Chem. Phys. 97 (1992) 2928.
[3] J. Titman, S. Feaux de la Croix, H.W. Spiess, J. Chem. Phys. 98 (1993) 3816.
[4] O.N. Antzutkin, S.C. Shekar, M.H. Levitt, J. Magn. Reson. A 115 (1995) 7.
[5] D.W. Alderman, G. McGeorge, J.Z. Hu, R.J. Pugmire, D.M. Grant, Molec. Phys. 95 (1998) 1113.
[6] St. Hesse, C. Jäger, Cellulose, submitted.
[7] J.Z. Hu, W. Wang, F. Liu, M.S. Solum, D.W. Alderman, R.J. Pugmire, D.M. Grant, J. Magn. Reson. A 133 (1995) 210.
[8] S.F. Liu, J.D. Mao, K. Schmidt-Rohr, J. Magn. Reson. 155 (2002) 15.
[9] R. Tycko, G. Dabbagh, P.A. Mirau, J. Magn. Reson. 85 (1989) 265.
[10] Y. Ishii, J. Ashida, T. Terao, Chem. Phys. Lett. 246 (1995) 439.
[11] M. Bak, J.T. Rasmussen, N.C. Nielsen, J. Magn. Reson. 147 (2000) 296.
[12] M. Bak, N.C. Nielsen, J. Mang. Reson. 125 (1997) 13.
[13] G.M. Brown, H.A. Levy, Acta Cryst. B 29 (1973) 790.
[14] M.H. Sherwood, D.W. Alderman, D.M. Grant, J. Magn. Reson. 104 (1993) 132.
[15] "Dmfit program": D. Massiot, F. Fayon, M. Capron, I. King, S. Le Calvé, B. Alonso, J.-O. Durand, B. Bujoli, Z. Gan, G. Hoatson, Magn. Reson. Chem. 40 (2002) 70.
[16] F.J. Kolpak, J. Blackwell, Macromolecules 9 (1976) 273.
[17] P. Langan, Y. Nishiyama, H. Chanzy, J. Am. Chem. Soc. 121 (1999) 9940.
[18] R.H. Atalla, D.L. VanderHart, Science 223 (1984) 283.
[19] D.L. VanderHart, R.H. Atalla, Macromolecules 17 (1984) 1465.
[20] D.L. VanderHart, R.H. Atalla, ACS Symp. Ser. 340 (1987) 88.
[21] J. Sugiyama, J. Persson, H. Chanzy, Macromolecules 24 (1991) 2461.
[22] J. Sugiyama, R. Vuong, H. Chanzy, Macromolecules 24 (1991) 4168.
[23] A. Lesage, M. Bardet, L. Emsley, J. Am. Chem. Soc. 121 (1999) 10987.
[24] T. Erata, T. Shikano, S. Yunoki, M. Takai, Cellulose Commun. 4 (1997) 128.
[25] H. Kono, S. Yunoki, T. Shikano, M. Fujiwara, T. Erata, M. Tkai, J. Am. Chem. Soc. 124 (2002) 7506.
[26] F.-Th. Koch, W. Prieß, R. Witter, U. Sternberg, Macromol. Chem. Phys. 201 (2000) 1930.
[27] U. Sternberg, F.T. Koch, W. Priess, R. Witter, Cellulose, submitted.